NLO QCD Corrections to the Production of Two Lepton Pairs via Vector-Boson Fusion at the LHC

Lucia Hošeková

7.9.2012

Particle Physics

"The electron is not as simple as it looks."

Sir William Lawrence Bragg

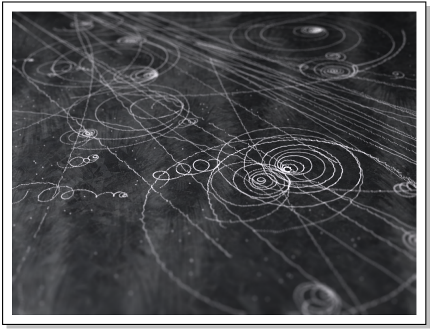

The Journey to the Standard Model

- 19th century - fundamental principles of nature were believed to be understood

> *"The more success the quantum theory has, the sillier it looks. "*
>
> Albert Einstein

- 20th century - Einstein's theory of relativity, emerging evidence of quantum mechanics undermined existing precepts of physics
- 1950's - "particle explosion": particle accelators unveiling large number of unpredicted and unexplained particles
- explosion of new theories and models followed, most importantly:
  - 1957 - electroweak interaction, γ, $W^{\pm}$ and Z boson as its carriers
  - quarks, colours and generations $\rightarrow$ QCD Lagrangian (1973)
  - gauge symmetry, Goldstone theorem, Higgs mechanism

The Standard Model

- a summary of our knowledge about three forces of nature tested for over 50 years

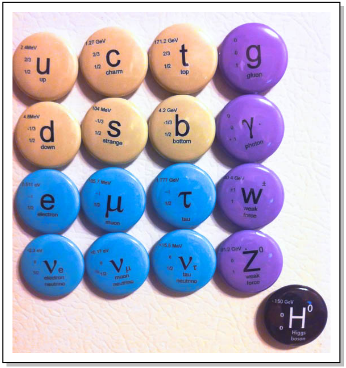

- fermions: form the 'ordinary matter'
    - quarks combine to form hadrons
    - leptons - no strong interactions
- gauge bosons: force carriers
    - gluons massless, mediate strong interactions and carry colour charge
    - W, Z are massive weak bosons mediating weak interaction
    - photon - massless stable gauge boson mediating electromagnetism
- all experimentally confirmed but one...

The Higgs Boson

- originates in the Higgs mechanism - current preferred theory of electroweak symmetry breaking
- massive and short-lived → direct observation not possible
- mass is not predicted by Standard Model

The Higgs Boson

- originates in the Higgs mechanism - current preferred theory of electroweak symmetry breaking
- massive and short-lived $\rightarrow$ direct observation not possible
- mass is not predicted by Standard Model

- July 4 2012 - ATLAS and CMS announcing a discovery of a new particle consistent with SM Higgs boson

Higgs Boson at the LHC

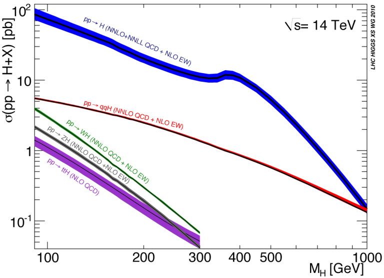

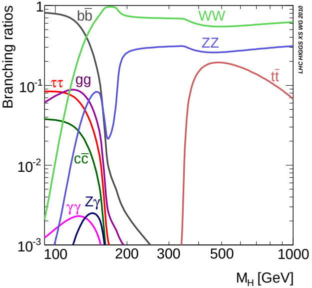

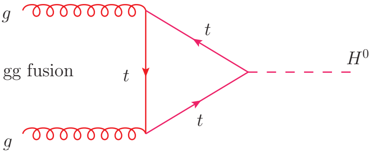

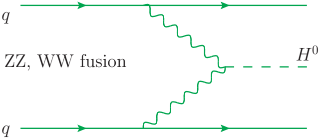

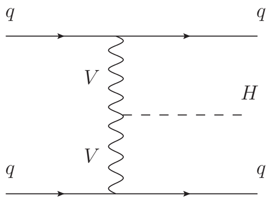

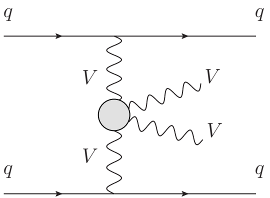

- why vector boson fusion?

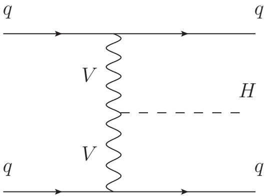

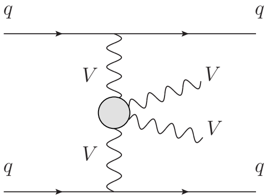

- why vector boson fusion?
  - one of the discovery modes for the SM Higgs boson (qq $\rightarrow$ qqH) with second largest cross section

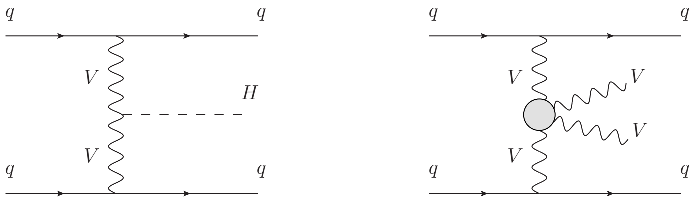

- why vector boson fusion?
  - one of the discovery modes for the SM Higgs boson (qq $\rightarrow$ qqH) with second largest cross section
  - testing characteristics of the Higgs
    - couplings to gauge bosons
    - CP properties

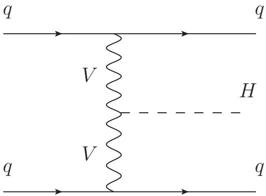

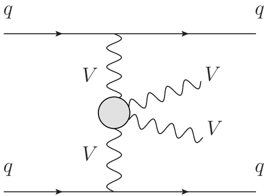

- why vector boson fusion?
  - one of the discovery modes for the SM Higgs boson (qq $\rightarrow$ qqH) with second largest cross section
  - testing characteristics of the Higgs
    - couplings to gauge bosons
    - CP properties
  - statistically significant thanks to forward jet tagging and suppressed QCD in the central region
  - (qq $\rightarrow$ qqVV) - background to H $\rightarrow$ VV decay mode via VBF

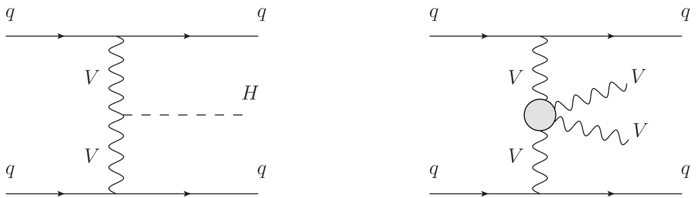

- why vector boson fusion?
  - one of the discovery modes for the SM Higgs boson (qq $\rightarrow$ qqH) with second largest cross section
  - testing characteristics of the Higgs
    - couplings to gauge bosons
    - CP properties
  - statistically significant thanks to forward jet tagging and suppressed QCD in the central region
  - (qq $\rightarrow$ qqVV) - background to H $\rightarrow$ VV decay mode via VBF
  - vector-boson scattering - important probe of EW symmetry breaking $\rightarrow$ door to new physics

Theoretical Studies

- 1980's - early results for pp→qqWW/ZZ - EW symmetry breaking studies
- 2000's - hadron collider studies for pp→qqVV→qq4l at LO and later NLO, resonant diagrams only
- NLO QCD corrections for full set of diagrams
  - includes non-resonant contributions
  - approximation - only includes *t*- and *u*-channel contribution

2006 -	Jäger, Oleari, Zeppenfeld:	$qq \to jjW^+W^- \to jj4l$
2006 -	Jäger, Oleari, Zeppenfeld:	$qq \to jjZZ \to jj4l$
2007 -	Bozzi, Jäger, Oleari, Zeppenfeld:	$qq \to jjWZ \to jj4l$
2009 -	Jäger, Oleari, Zeppenfeld:	$qq \to jjW^\pm W^\pm \to jj4l$

Generic Processes

$pp \to jjW^+W^+$	$uc \to dse^+\nu_e\mu^+\nu_\mu$	$pp \to jjW^-W^-$	$ds \to uce^-\bar{\nu}_e\mu^-\bar{\nu}_\mu$
$pp \to jjW^+Z$	$uc \to dce^+\nu_e\mu^+\mu^-$	$pp \to jjZZ$	$ds \to dse^+e^-\mu^+\mu^-$
	$us \to dse^+\nu_e\mu^+\mu^-$		$uc \to uce^+e^-\mu^+\mu^-$
$pp \to jjW^-Z$	$dc \to uce^-\bar{\nu}_e\mu^+\mu^-$		$us \to use^+e^-\mu^+\mu^-$
	$ds \to use^-\bar{\nu}_e\mu^+\mu^-$		$us \to dce^+e^-\mu^+\mu^-$
$pp \to jjW^+W^-$	$ds \to dse^+\nu_e\mu^-\bar{\nu}_\mu$		$ds \to dse^+e^-\nu_\mu\bar{\nu}_\mu$
	$uc \to uce^+\nu_e\mu^-\bar{\nu}_\mu$		$uc \to uce^+e^-\nu_\mu\bar{\nu}_\mu$
	$us \to use^+\nu_e\mu^-\bar{\nu}_\mu$		$us \to use^+e^-\nu_\mu\bar{\nu}_\mu$
	$us \to dce^+\nu_e\mu^-\bar{\nu}_\mu$		$us \to dce^+e^-\nu_\mu\bar{\nu}_\mu$

- all remaining subprocesses can be derived from the generic ones
- each subprocess - up to 600 diagrams at LO
- $uc \to dse^+\nu_e\mu^+\nu_\mu$: 93 Born diagrams, 452 real radiation diagrams, 430 one-loop diagrams and 346 counterterm diagrams

Partonic subprocesses for $uc \to ds\, W^+W^+ \;\to\; ds\, e^+\nu_e\mu^+\nu_\mu$

$QQ \to QQ\mathrm{e}^+\nu_\mathrm{e}\mu^+\nu_\mu$	$\bar{Q}Q \to \bar{Q}Q\mathrm{e}^+\nu_\mathrm{e}\mu^+\nu_\mu$	$Q\bar{Q} \to \bar{Q}Q\mathrm{e}^+\nu_\mathrm{e}\mu^+\nu_\mu$
$\mathrm{uc} \to \mathrm{dse}^+\nu_\mathrm{e}\mu^+\nu_\mu$	$\bar{\mathrm{d}}\mathrm{c} \to \bar{\mathrm{u}}\mathrm{se}^+\nu_\mathrm{e}\mu^+\nu_\mu$	$\mathrm{c}\bar{\mathrm{d}} \to \bar{\mathrm{u}}\mathrm{se}^+\nu_\mathrm{e}\mu^+\nu_\mu$
$\mathrm{cu} \to \mathrm{dse}^+\nu_\mathrm{e}\mu^+\nu_\mu$	$\bar{\mathrm{s}}\mathrm{u} \to \bar{\mathrm{c}}\mathrm{de}^+\nu_\mathrm{e}\mu^+\nu_\mu$	$\mathrm{u}\bar{\mathrm{s}} \to \bar{\mathrm{c}}\mathrm{de}^+\nu_\mathrm{e}\mu^+\nu_\mu$
$\mathrm{uu} \to \mathrm{dde}^+\nu_\mathrm{e}\mu^+\nu_\mu$	$\bar{\mathrm{d}}\mathrm{u} \to \bar{\mathrm{u}}\mathrm{de}^+\nu_\mathrm{e}\mu^+\nu_\mu$	$\mathrm{u}\bar{\mathrm{d}} \to \bar{\mathrm{u}}\mathrm{de}^+\nu_\mathrm{e}\mu^+\nu_\mu$
$\mathrm{cc} \to \mathrm{sse}^+\nu_\mathrm{e}\mu^+\nu_\mu$	$\bar{\mathrm{s}}\mathrm{c} \to \bar{\mathrm{c}}\mathrm{se}^+\nu_\mathrm{e}\mu^+\nu_\mu$	$\mathrm{c}\bar{\mathrm{s}} \to \bar{\mathrm{c}}\mathrm{se}^+\nu_\mathrm{e}\mu^+\nu_\mu$
$\bar{Q}\bar{Q} \to \bar{Q}\bar{Q}\mathrm{e}^\pm\nu_\mathrm{e}\mu^\pm\nu_\mu$	$\bar{\mathrm{d}}\mathrm{u} \to \bar{\mathrm{c}}\mathrm{se}^+\nu_\mathrm{e}\mu^+\nu_\mu$	$\mathrm{u}\bar{\mathrm{d}} \to \bar{\mathrm{c}}\mathrm{se}^+\nu_\mathrm{e}\mu^+\nu_\mu$
$\bar{\mathrm{d}}\bar{\mathrm{s}} \to \bar{\mathrm{u}}\bar{\mathrm{c}}\mathrm{e}^+\nu_\mathrm{e}\mu^+\nu_\mu$	$\bar{\mathrm{s}}\mathrm{c} \to \bar{\mathrm{u}}\mathrm{de}^+\nu_\mathrm{e}\mu^+\nu_\mu$	$\mathrm{c}\bar{\mathrm{s}} \to \bar{\mathrm{u}}\mathrm{de}^+\nu_\mathrm{e}\mu^+\nu_\mu$
$\bar{\mathrm{s}}\bar{\mathrm{d}} \to \bar{\mathrm{u}}\bar{\mathrm{c}}\mathrm{e}^+\nu_\mathrm{e}\mu^+\nu_\mu$		
$\bar{\mathrm{d}}\bar{\mathrm{d}} \to \bar{\mathrm{u}}\bar{\mathrm{u}}\mathrm{e}^+\nu_\mathrm{e}\mu^+\nu_\mu$		
$\bar{\mathrm{s}}\bar{\mathrm{s}} \to \bar{\mathrm{c}}\bar{\mathrm{c}}\mathrm{e}^+\nu_\mathrm{e}\mu^+\nu_\mu$		

Classification of Diagrams

Kinematic channels:

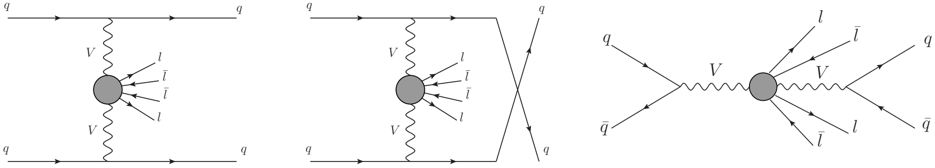

Additional topologies:

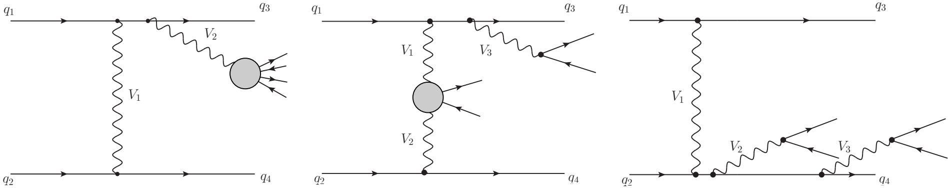

Structure of Diagrams

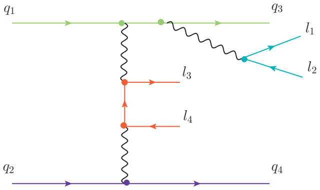

Structure of Diagrams

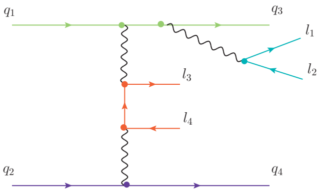

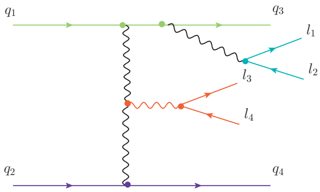

Structure of Diagrams

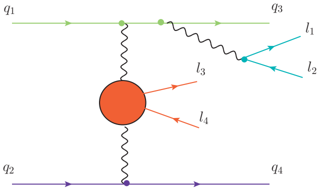

Structure of Diagrams

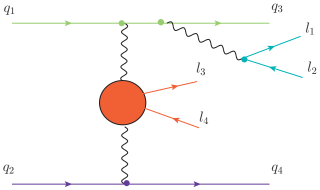

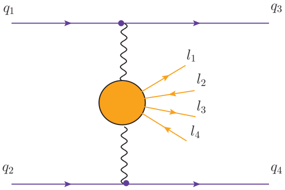

Structure of Diagrams

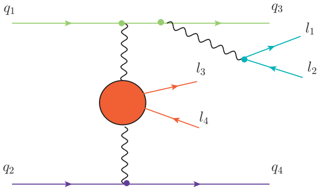

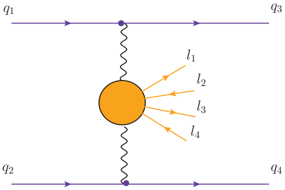

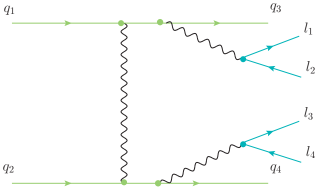

Structure of Diagrams

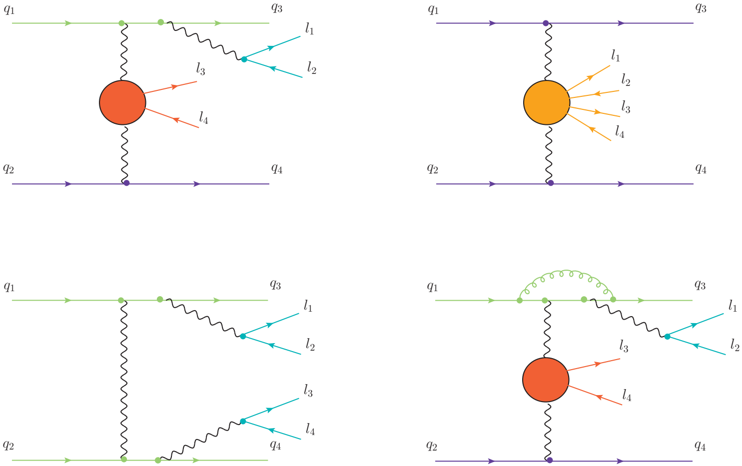

Modular Structure

- small number of building blocks can be used to construct large number of diagrams
- QCD NLO corrections have no effect on EW blocks
- separating QCD and EW blocks
    - blocks can be recycled across diagrams, subprocesses and perturbative orders
    - more effective and faster code

Modular Structure

- small number of building blocks can be used to construct large number of diagrams
- QCD NLO corrections have no effect on EW blocks
- separating QCD and EW blocks
  - blocks can be recycled across diagrams, subprocesses and perturbative orders
  - more effective and faster code
- insert $g^{\mu\nu} = -\sum_{i=\{+,-,0\}} \varepsilon(k)_i^{\mu} \varepsilon^*(k)_i^{\nu} + \frac{k^\mu k^\nu}{k^2}$ into propagators $\frac{-\mathrm{i}g^{\mu\nu}}{p^2-m^2+\mathrm{i}\varepsilon}$
- with off-shell polarization vectors ($m \mapsto \sqrt{k^2}$)
- for $\varepsilon_p^{\mu}(k) = \frac{k^\mu}{\sqrt{k^2}}$, $\varepsilon_p^{*\mu}(k) = -\frac{k^\mu}{\sqrt{k^2}}$ we get

$$g^{\mu\nu} = -\sum_{i=\{+,-,0,p\}} \varepsilon_i^{\mu}(k)\varepsilon_i^{*\nu}(k)$$

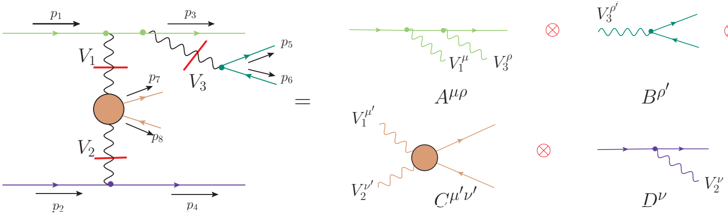

$$-\sum_{i,j,k=\{\pm,0,p\}} [A^{\mu\rho}\varepsilon^*_{1,i,\mu}(k_1)\varepsilon^*_{3,k,\rho}(k_3)]\ [B^{\rho'}\varepsilon_{3,k,\rho'}(k_3)][C^{\mu'\nu'}\varepsilon_{1,i,\mu'}(k_1)\varepsilon_{2,j,\nu'}(k_2)]\ [D^\nu\varepsilon^*_{2,j,\nu}(k_2)]$$

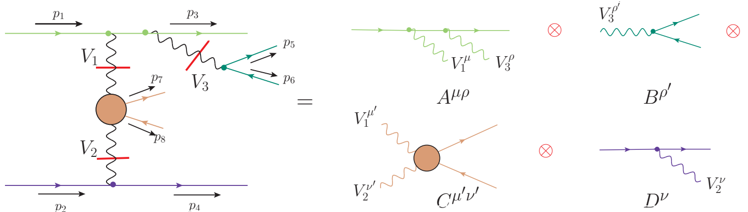

$$-\sum_{i,j,k=\{\pm,0,p\}} [A^{\mu\rho}\varepsilon^*_{1,i,\mu}(k_1)\varepsilon^*_{3,k,\rho}(k_3)]\ [B^{\rho'}\varepsilon_{3,k,\rho'}(k_3)][C^{\mu'\nu'}\varepsilon_{1,i,\mu'}(k_1)\varepsilon_{2,j,\nu'}(k_2)]\ [D^{\nu}\varepsilon^*_{2,j,\nu}(k_2)]$$

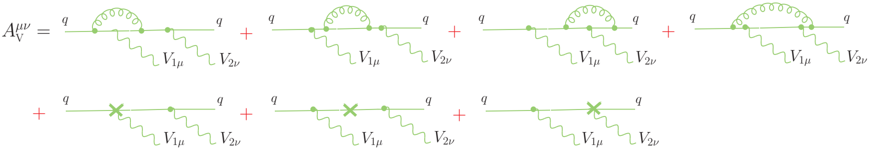

Dipole subtraction method

$$\sigma = \int_m d\sigma^B + \int_{m+1} d\sigma^R + \int_m d\sigma^V$$

- $d\sigma^B$: Born cross-section - no singularities
- $d\sigma^R$: real cross-section - collinear and soft singularities
- $d\sigma^V$: virtual cross-section - IR singularities
- singularities in σ^R and σ^V cancel each other
- analytical integration not possible
- dipole subtraction Catani, Seymour (1997)

$$\sigma^{NLO} = \int_{m+1} (d\sigma^R - d\sigma^A) + \int_m (d\sigma^V + \int_1 d\sigma^A)$$

- $d\sigma^A$: subtraction term containing all IR singularities and analytically integrable over 1-particle phase-space causing collinear and soft singularities

NLO cross section

$$\sigma^{\mathrm{NLO}}_{\mathrm{pp}} = \sum_{a,b} \int_0^1 \mathrm{d}x_1 \int_0^1 \mathrm{d}x_2\, f_a^{\mathrm{NLO}}(x_1,\mu_{\mathrm{F}}) f_b^{\mathrm{NLO}}(x_2,\mu_{\mathrm{F}})$$
$$\times \Bigg\{ \int_m \mathrm{d}\Phi_m \Big[\mathrm{d}\hat{\sigma}^{\mathrm{B}}_{ab}(x_1p_1, x_2p_2) + \mathrm{d}\hat{\sigma}^{\mathrm{V}}_{ab}(x_1p_1, x_2p_2) + \mathbf{I}\otimes \mathrm{d}\hat{\sigma}^{\mathrm{B}}_{ab}(x_1p_1, x_2p_2)\Big]$$
$$+ \int_0^1 \mathrm{d}z_1 \int_m \mathrm{d}\Phi_m \left(\mathbf{K}_{aa'}(z_1) + \mathbf{P}_{aa'}(z_1)\right) \otimes \mathrm{d}\hat{\sigma}^{\mathrm{B}}_{a'b}(z_1x_1p_1, x_2p_2)$$
$$+ \int_0^1 \mathrm{d}z_2 \int_m \mathrm{d}\Phi_m \left(\mathbf{K}_{bb'}(z_2) + \mathbf{P}_{bb'}(z_2)\right) \otimes \mathrm{d}\hat{\sigma}^{\mathrm{B}}_{ab'}(x_1p_1, z_2x_2p_2)$$
$$+ \int_{m+1} \mathrm{d}\Phi_{m+1} \left(\mathrm{d}\hat{\sigma}^{\mathrm{R}}_{ab}(x_1p_1, x_2p_2) - \sum_{\mathrm{dipoles}} \left(\mathrm{d}V_{\mathrm{dipole}} \otimes \mathrm{d}\hat{\sigma}^{\mathrm{B}}_{ab}\right)(x_1p_1, x_2p_2) \right) \Bigg\}$$

Numerical Evaluation

- EW and QCD blocks with FeynArts + FormCalc Hahn, Perez-Victoria
- Weyl-van der Waerden helicity formalism Dittmaier (1998)
    - translates all kinematic objects into two-component WvdW spinors in chiral representation
    - numerical evaluation of all building blocks
- Mathematica code modified for polarization sum insertions, exported to Fortran
- virtual corrections
    - contain up to 5-point functions
    - tensor reduction performed in Fortran by COLLIER library Denner, Dittmaier, Hofer
    - supports both mass and dimensional regularization
- returns arrays of full squared amplitudes for each subprocess, called from within Monte Carlo

Numerical Checks

- tree-level ME's compared with Madgraph (10^{-8}), FormCalc (10^{-16})
- virtual ME's compared with LoopTools (10^{-6}), subtraction of IR poles checked (10^{-16})
- comparison with Jäger, Oleari, Zeppenfeld: arXiv:0907.0580v2

PDF set	σ[fb]	σ_{JOZ}[fb]	δ[%]
CTEQ6L1 (LO)	1.4746(7)	1.478	$-0.23(5)$
MSTW08 (LO)	1.4061(7)	1.409	$-0.21(5)$
CTEQ6M (NLO)	1.405(1)	1.404	$+0.10(9)$
MSTW08 (NLO)	1.372(1)	1.372	$-0.00(9)$

- comparison with Jäger, Zanderighi: arXiv:1108.0864v2

PDF set	σ[fb]	σ_{JZ}[fb]	δ[%]
MSTW08 (NLO)	0.1961(2)	0.201(3)	-2.3(1.5)

Setup

- results from Denner, Hošeková, Kallweit - arXiv:1209.2389
- neglecting fermion masses, t and b quark, CKM approximated by unit matrix
- complex mass scheme - $M_V^{\mathrm{CMS}} = \sqrt{M_V^2 - \mathrm{i} M_V \Gamma_V}$ throughout
- tree-level contributions generated using OpenLoops (Cascioli, Maierhöfer, Pozzorini - arXiv:1111.5206)
- VBF cuts
  - tagging jets - two hard reconstructed jets with $p_T \geq 20$ GeV, large rapidity separation $\triangle y_{jj} > 4$ and invariant mass $M_{jj} > 600$ GeV
  - separation of jets and leptons $\triangle R_{ll} > 0.2$, $\triangle R_{jl} > 0.4$, leptons in between jets in rapidity
- two scale choices:

$$\mu_{\mathrm{F}} = \mu_{\mathrm{R}} = \xi M_{\mathrm{W}} \qquad \mu_{\mathrm{F}} = \mu_{\mathrm{R}} = \xi \sqrt{p_{\mathrm{T,jet_1}} \cdot p_{\mathrm{T,jet_2}}}$$

Scale Dependence

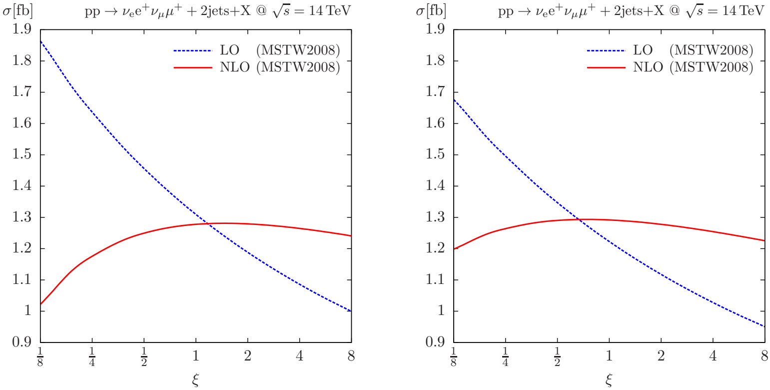

(a) $\mu_F = \mu_R = \xi M_W$

(b) $\mu_F = \mu_R = \xi \sqrt{p_{T,jet_1} \cdot p_{T,jet_2}}$

- $1/2 < \xi < 2$ - LO scale variation 10%, NLO is 2% for FS and 1% for DS

Integrated cross section

- estimating the size of *s*-channel and interference contributions using VBF cuts

ξ	σ^{LO}_{full} [fb]	$\sigma^{LO}_{VBF+int}$ [fb]	σ^{LO}_{VBF} [fb]	σ^{NLO}_{VBF} [fb]
1/8	1.6763(2)	1.6755(2)	1.6771(2)	1.198(2)
1/4	1.4956(2)	1.4949(2)	1.4964(2)	1.264(1)
1/2	1.3467(2)	1.3461(2)	1.3474(2)	1.2903(9)
1	1.2224(2)	1.2218(2)	1.2230(2)	1.2917(8)
2	1.1173(2)	1.1168(2)	1.1179(2)	1.2778(7)
4	1.0275(2)	1.0270(2)	1.0280(2)	1.2544(6)
8	0.9499(2)	0.9494(2)	0.9504(2)	1.2253(6)

- interferences contribute -0.05% and *s*-channel diagrams 0.1% of the LO cross section

Jet Transverse Momentum

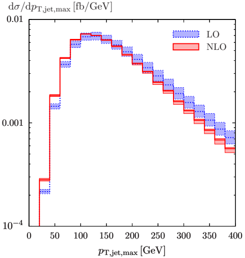

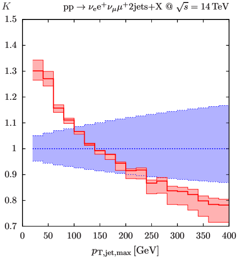

$\mu_F = \mu_R = \xi M_W$

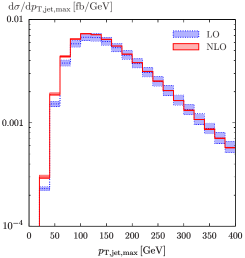

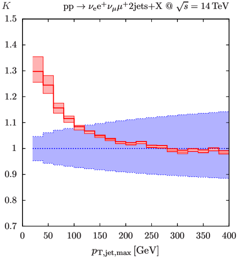

$\mu_F = \mu_R = \xi \sqrt{p_{T,\mathrm{jet}_1} \cdot p_{T,\mathrm{jet}_2}}$

Jet Rapidity

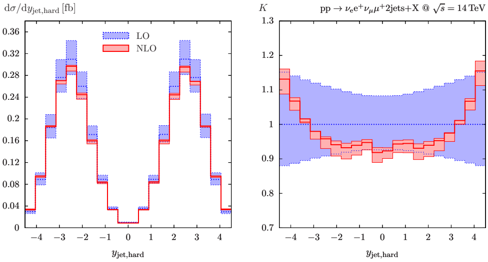

$\mu_F = \mu_R = \xi M_W$

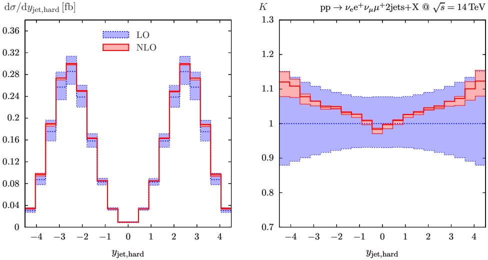

$\mu_F = \mu_R = \xi \sqrt{p_{T,jet_1} \cdot p_{T,jet_2}}$

Invariant Mass of Two Jets

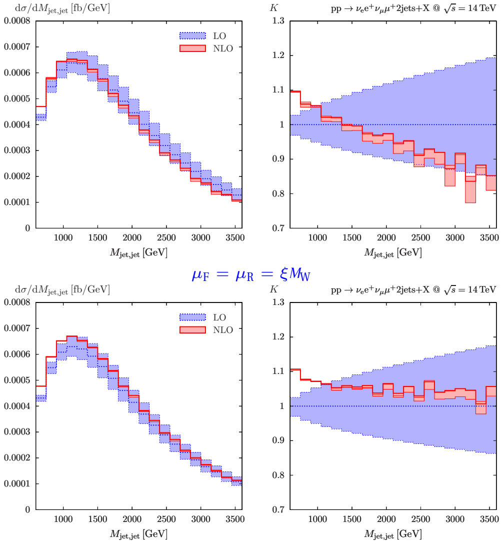

$$\mu_F = \mu_R = \xi\sqrt{p_{T,jet_1} \cdot p_{T,jet_2}}$$

Azimuthal Angle Between Leptons

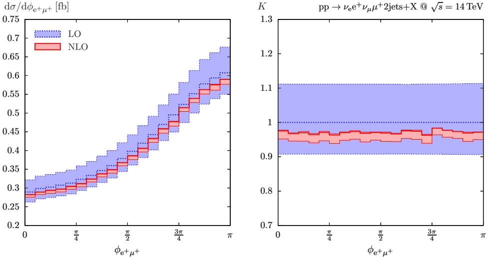

$\mu_F = \mu_R = \xi M_W$

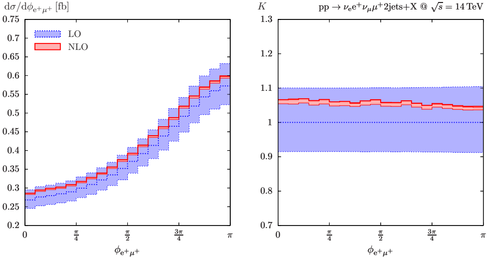

$\mu_F = \mu_R = \xi \sqrt{p_{T,jet_1} \cdot p_{T,jet_2}}$

Summary

- vector-boson fusion at hadron colliders
  - irreducible background to Higgs boson production at the LHC
  - probe into EW symmetry breaking
- full NLO corrections are fairly complicated (many legs, large number of diagrams) and require modular approach
- independent verification of the existing calculation of W^+W^+ production, introducing new scale and numerical assessment of the neglected s channel and interferences for VBF cuts
- QCD corrections below 10% of the LO cross section in distributions
- higher order uncertainty 1% for $\mu_F = \mu_R = \xi\sqrt{p_{T,\mathrm{jet}_1} \cdot p_{T,\mathrm{jet}_2}}$
- outlook - numerical results for the remaining production modes

Thank you.

Backup - EW symmetry breaking

- the scattering of longitudinal W's grows with energy and violates unitarity

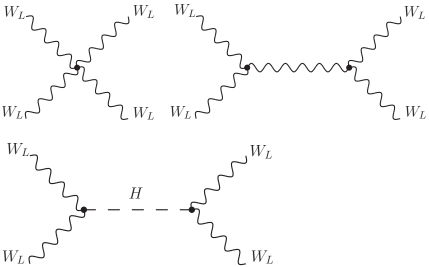

$$\propto g_W^2 \frac{E^2}{M_W^2}$$

$$\propto -g_W^2 \frac{E^2}{M_W^2}$$

- without Higgs, new mechanism of EW symmetry breaking must be considered
- new physics (composite Higgs, extra dimensions,...) predicts new resonances and modify VBF
- qq $\rightarrow$ qqWW very sensitive channel to new interaction
- minimizes the background from transversely polarized WW

Backup - Tree-level studies

- first partial results Cahn, Dawson (1984)
- pp→qqWW in effective gauge boson approximation, only for longitudinal polarization Duncan, Kane, Repko (1986)
- exact calculation of pp→qqWW, all polarizations Dicus, Vega (1986)
- pp→qqZZ, effective gauge boson approximation Abbasabadi, Repko (1988)
- pp→qqZZ→qqllll, narrow width approximation Baur, Glover (1990)
- pp→(qqZW→qqZW)+X, effective gauge boson approximation, longitudinal polarization Dobado, Herrero, Terron (1991)
- pp→qqZW, full tree-level, leptonic decay correlations Barger, Cheung, Han, Stange, Zeppenfeld (1992)
- pp→qqWW - electroweak chiral lagrangian formalism, semileptonic decay Butterworth, Cox, Forshaw (2002)
- pp→qqllll - complete parton level analysis, SM and SILH Ballestrero, Accomando, Bevilacqua, Franzosi, Maina (2006-2010)
- multiple BSM studies for the LHC Han, Krohn, Wang, Zhu (2009), Cheung, Chiang, Yuan (2008)...

Backup - Diagrams - NLO QCD Contributions

Virtual corrections

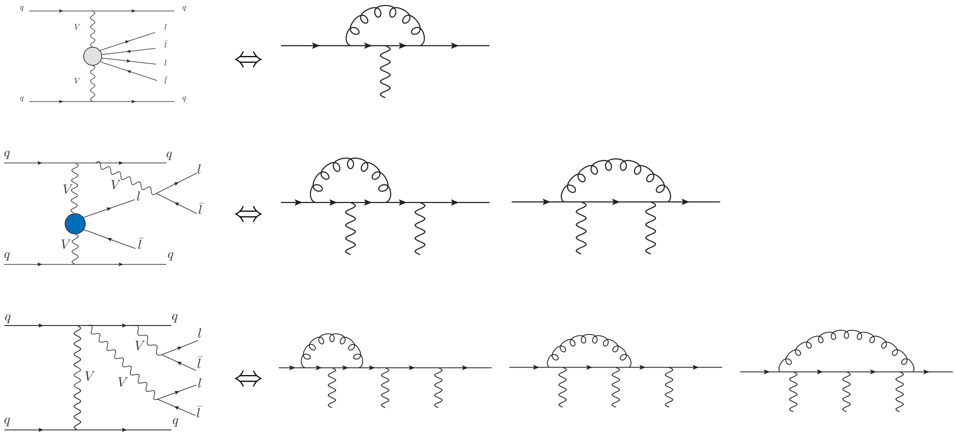

Counterterms

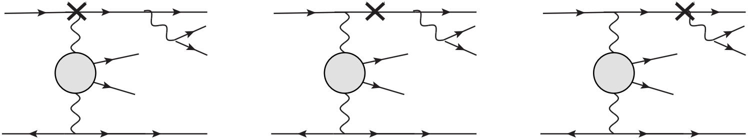

,...

Real corrections

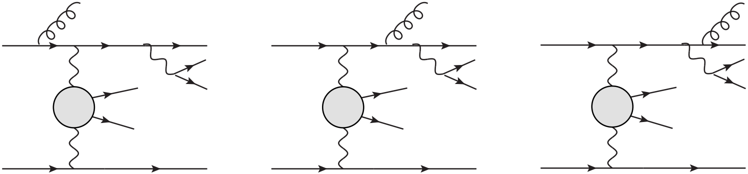

,...

Initial state gluon

- spacelike gauge bosons

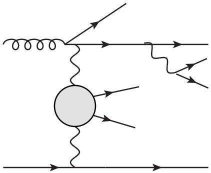
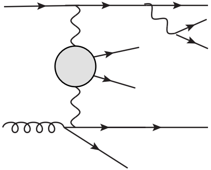

- timelike gauge bosons

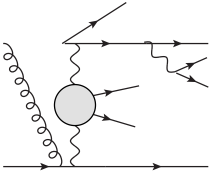
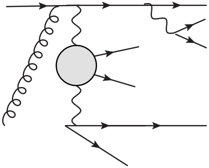

(PL = 6 = +)

1. WvdW spinors

$$\bar{\Psi}(k_2)P_R\gamma^{\mu}\Psi(k_3) \mapsto k_2^a \sigma^{\mu}_{a\dot{b}} k_3^{\dot{b}}$$

2. open Lorentz indices contracted (polarization sum)

$$k_2^a \sigma^{\mu}_{a\dot{b}} k_3^{\dot{b}} \mapsto k_2^a \varepsilon_{\mu+}(k_1) \sigma^{\mu}_{a\dot{b}} k_3^{\dot{b}}$$

3. scalar products of individual spinors

$$k_2^a \varepsilon_{\mu+}(k_1) \sigma^{\mu}_{a\dot{b}} k_3^{\dot{b}} \mapsto 2\sqrt{2k_0(2)k_0(3)}\langle n_2(1)n_1(3)\rangle(n_1(1)n_1(2))$$

2 Sqrt[2] barprod[n1[3], n2[1]] Sqrt[k0[2]] Sqrt[k0[3]] prod[n1[2], n1[1

4. full forms of spinors are introduced

$$(n_1(1)n_1(2)) = (\sin\frac{\theta(1)}{2}, -e^{-\mathrm{i}\Phi(1)}\cos\frac{\theta(1)}{2}).\begin{pmatrix} e^{-\mathrm{i}\Phi(2)}\cos\frac{\theta(2)}{2} \\ \sin\frac{\theta(2)}{2}) \end{pmatrix}$$

5. s- and u-channel obtained via crossing which amounts to sign reversal of certain spinors